

Aberration-Corrected Imaging of Active Sites on Industrial Catalyst Nanoparticles**

Lionel Cervera Gontard, Lan-Yun Chang, Crispin J. D. Hetherington, Angus I. Kirkland, Dogan Ozkaya, and Rafal E. Dunin-Borkowski*

The active components of industrial heterogeneous catalysts are often small metallic particles, whose reactivity and selectivity depend on the presence of steps and kinks on their surfaces. Although scanning probe microscopy can be used to identify the roles of active sites on the extended surfaces of model catalysts, little is known about atomic arrangements on the surfaces of commercial catalyst nanoparticles, as highlighted by a recent study of ammonia synthesis in a Ru-catalyzed reaction.^[1] High-resolution transmission electron microscopy (HRTEM) has been used extensively to characterize such particles.^[2] However, conventional HRTEM images are affected by electron microscope objective lens aberrations, limiting spatial resolution, and complicating interpretation. The visibility of nanoparticles can also be affected by strong phase contrast from their support.^[3]

Here, we show that spherical-aberration-corrected transmission electron microscopy (TEM) can be used to provide atomic-resolution information about the local topologies of active sites on commercial nanoparticles with greatly improved sensitivity. We used two advanced TEM techniques, which are based on recent developments in hardware (aberration correction)^[4] and computation (exit wavefunction restoration),^[5] to examine a powder of Pt nanoparticles on carbon black, which had been heated to 900 °C in a N₂-rich atmosphere. These particles are used to both electrooxidize H₂ and electroreduce O₂ at the anode and cathode, respectively, of a polymer electrolyte membrane fuel cell. Figure 1 A

shows the measured phase of the specimen exit surface wavefunction of a representative Pt nanoparticle, determined in the present study from a focal series of aberration-corrected images acquired using a JEM-2200FS transmission electron microscope, viewed close to a $\langle 110 \rangle$ direction. Despite the presence of a graphitic carbon support, terraces and steps around the edge of the particle are visible directly with a sensitivity, visibility, and spatial resolution that are improved greatly over those in a conventional high-resolution TEM image. The monatomic steps that are visible in Figure 1 A are conventionally termed A or B type, with either $\{100\}$ or $\{111\}$ microfacet risers that have different catalytic properties. The heights of the peaks in Figure 1 A are related to the number of atoms in each atomic column and can be used to obtain information about the atomic arrangement on each of the surfaces that is viewed in cross section. In contrast to the atomic arrangements that have been suggested by homoepitaxial growth experiments on extended Pt surfaces, our results, which are consistent between different Pt particles (Figure 2), provide compelling evidence that the outermost atomic layers consist of irregular islands of atoms. Figure 3 illustrates the improvement obtained by recovering the specimen exit wavefunction over the information present in a single HRTEM image. The power spectra shown below each image in Figure 3 show the presence of higher-spatial-resolution lattice fringe information in the reconstructed image and the decreased contribution to the power spectrum from amorphous carbon.

Figure 1 B shows a simulated phase image, calculated from the model shown in Figure 1 C, which is consistent with the experimental image shown in Figure 1 A. Although the relative alignment of adjacent columns in the electron beam direction cannot be determined uniquely from Figure 1 A alone, the nature of the roughness of the terraces shown in Figure 1 B,C is clear. Multislice simulations of the amplitude and phase of the exit wavefunction, in which the surface of the particle was modified by adding or removing atoms, were performed for a range of models of the particle (Figure 4) until a best fit to the experimental image was obtained. In the simulations, the phase images were band-pass-filtered using a cut-off frequency equal to the maximum spatial frequency present in the experimental image. The best-fitting model shown in Figure 1 C suggests that steps on the $\{100\}$ facets of this particle are largely straight, while kinks and step vacancies are present on the $\{111\}$ facets.

We anticipate that the ability to obtain results such as those shown in Figures 1–3, especially in a gas reaction environment and in combination with electron tomography, will contribute to the design and development of improved

[*] L. C. Gontard, Prof. R. E. Dunin-Borkowski
Department of Materials Science and Metallurgy
University of Cambridge
Pembroke Street, Cambridge CB23QZ (UK)
Fax: (+44) 1223-33-4567
E-mail: rdb@cen.dtu.dk
Homepage: <http://www.rafaledb.com/>

Dr. L.-Y. Chang, Dr. C. J. D. Hetherington, Prof. A. I. Kirkland
Department of Materials
University of Oxford
Parks Road, Oxford OX1 3PH (UK)

Dr. D. Ozkaya
Johnson Matthey Technology Centre
Blount's Court, Sonning Common, Reading RG4 9NH (UK)

Prof. R. E. Dunin-Borkowski
Center for Electron Nanoscopy
Technical University of Denmark
2800 Kongens Lyngby (Denmark)

[**] L.C.G. acknowledges P. Ash and D. Thompsett from the Johnson Matthey Technology Centre, Reading (UK), for valuable discussions, provision of samples, and financial support. The authors are grateful to the EPSRC and the Royal Society for financial support.

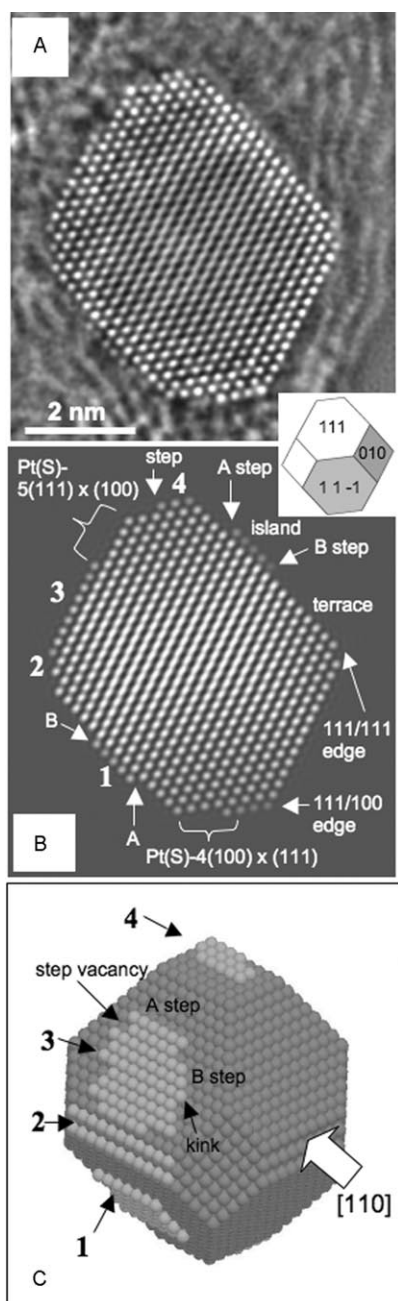


Figure 1. A) Restored phase of a 6-nm Pt particle obtained by applying spherical aberration correction and through-focus exit wavefunction restoration to a defocus series of 20 images acquired at 200 kV with the coefficient of spherical aberration, C_s , adjusted to $-30 \mu\text{m}$. B) Best-fitting simulated phase. C) Three-dimensional atomic model used to calculate the best-fitting phase in part (B). The large white arrow indicates the direction of the electron beam. The inset overlapping parts (A, B) shows the crystallographic details of the particle. In parts (B, C), 1–4 correspond to the same features on the surface of the particle. The notation $\text{Pt(S)}-n(x,y,z) \times (u,v,w)$ refers to the micro-facets, on which n is the number of atoms in the terrace, (x,y,z) is the Miller index of the terrace, and (u,v,w) is the Miller index of the step.

catalysts, as well as providing valuable input to studies in surface chemistry and theoretical modeling. For example, it has been reported that O_2 molecules dissociate more easily at

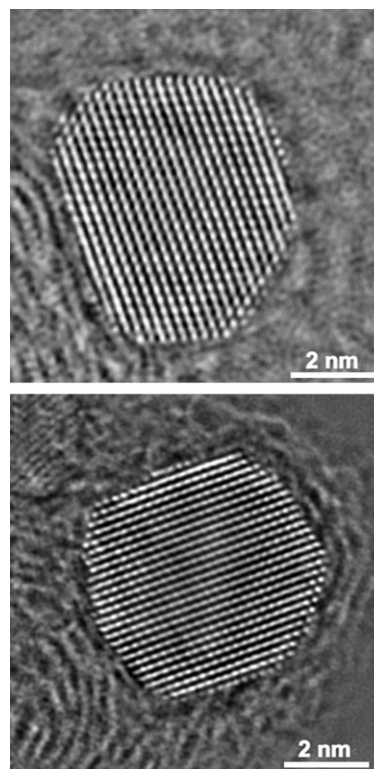


Figure 2. Phase images recorded from Pt particles similar to that shown in Figure 1 A.

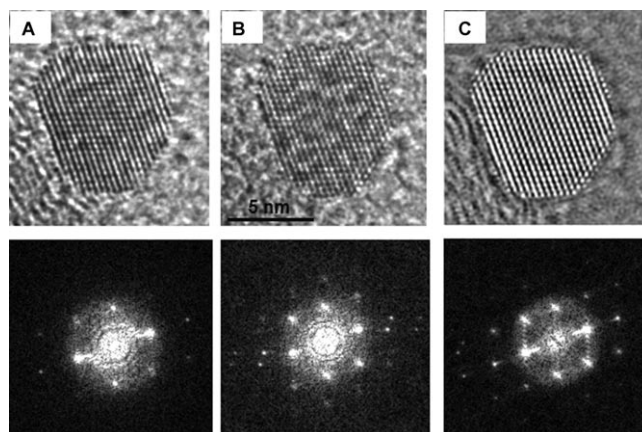


Figure 3. A, B) HRTEM (intensity) images of the Pt particle shown in Figure 2A, acquired with C_s adjusted to 0.5 mm (A) and $-30 \mu\text{m}$ (B). Corresponding power spectra are shown beneath each image. C) Phase image and power spectrum of the same particle, obtained by applying exit wavefunction restoration to a through-focus series of aberration-corrected images.

steps on Pt(111) facets than at other sites, while H_2 has been reported to dissociate more readily on B-type than on A-type steps at room temperature.^[6,7]

A final important factor that affects the catalytic stability of nanoparticle clusters is the strength of their anchorage to their support. All of the catalyst particles that were examined were highly stable under the electron beam, indicating that they are anchored strongly to their carbon support, which is

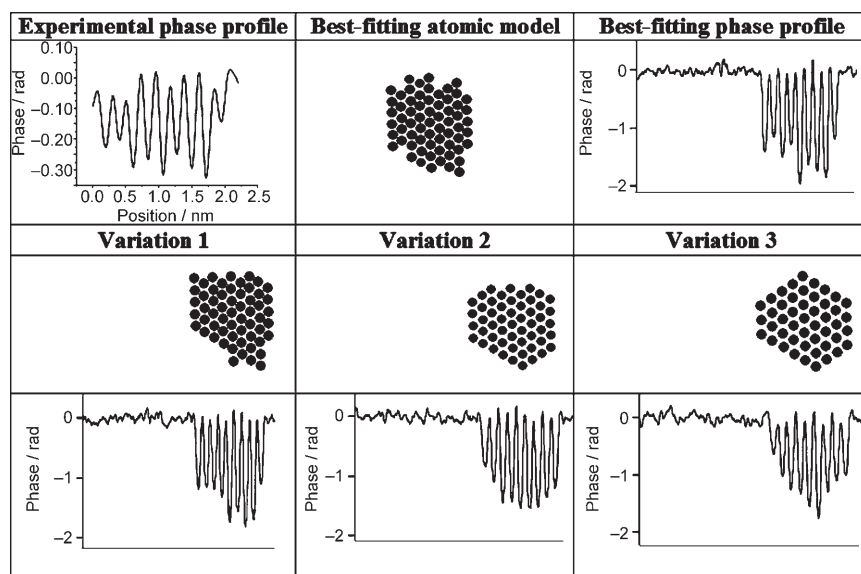


Figure 4. Selected examples taken from the procedure used to find a best-fitting model to the shape of island 3 shown in Figure 1. The magnitudes of the simulated phase shifts, both on the terraces and in the center of the particle, are higher in the simulations than in the experimental data. This difference may provide insight into the poorly understood discrepancy between the contrast of simulated and experimental conventional HRTEM images, known as the Stobbs factor. Profiles 1, 2, and 3 highlight the sensitivity of the phase profiles to the number of atoms in each column.

graphitized locally in the vicinity of each particle. In Figure 3C, the graphitic planes in the support are better defined after exit wavefunction restoration and provide improved information about how the particle contacts graphene layers at a 111-type facet. Steps on Pt surfaces are known to be active for H–H and C–H bond breaking, while kinks at steps are also active for C–C bond breaking.^[8] The

high density of kinks that we observe on (111) facets may provide an explanation for the strong anchoring of the particles to their support. Furthermore, the selectivity of steps and kinks for C–C bond breaking may prevent poisoning of the particle by carbon from the support.

Received: November 27, 2006

Published online: March 23, 2007

Keywords: active sites · electron microscopy · heterogeneous catalysis · nanoparticles · platinum

- [1] K. Honkala, A. Hellman, I. N. Remiadakis, A. Logadottir, A. Carlsson, S. Dahl, C. H. Christensen, J. K. Nørskov, *Science* **2005**, 307, 555–558.
- [2] L. D. Marks, D. J. Smith, *Nature* **1983**, 303, 316–317.
- [3] A. K. Datye, A. D. Logan, J. Blankenburg, D. J. Smith, *Ultramicroscopy* **1990**, 34, 47–53.
- [4] M. Haider, H. Rose, S. Uhlemann, E. Schwan, B. Kabius, K. Urban, *Ultramicroscopy* **1998**, 75, 53–60.
- [5] A. I. Kirkland, R. R. Meyer, *Microsc. Microanal.* **2004**, 10, 401–413.
- [6] P. Gambardella, Z. Sljivancanin, B. Hammer, M. Blanc, K. Kuhnke, K. Kern, *Phys. Rev. Lett.* **2001**, 87, 056103.
- [7] B. Lang, R. W. Joyner, G. A. Somorjai, *Surf. Sci.* **1972**, 30, 454–474.
- [8] D. W. Blakely, G. A. Somorjai, *J. Catal.* **1976**, 42, 181–196.